16th World Conference on Earthquake, 16WCEE 2017
Santiago Chile, January 9th to 13th 2017
Paper N° 1341
Registration Code: S-N1442215191

EVALUATION METHOD OF SEISMIC DEFORMATION FOR AIRPORT BASIC FACILITIES ON GRID-TYPE IMPROVED GROUND

Y. Saeki[1], Y. Ohya[2], E. Kohama[3], and S. Sato[4]

[1] Engineer, Aviation Department, Pacific Consultants Co.,Ltd., Tokyo, Japan, yoshitaka.saeki@ss.pacific.co.jp
[2] Senior Researcher, Port and Airport Research Institute, Yokosuka, Japan, ooya-y@pari.go.jp
[3] Head of Group, Port and Airport Research Institute, Yokosuka, Japan, kohama-e83ab@pari.go.jp
[4] Engineer, Seismic Design Center, Pacific Consultants Co.,Ltd., Tokyo, Japan, shigeru.satou@tk.pacific.co.jp

Abstract

A method of evaluating deformation of asphalt pavements on the ground improved by grid-type improvement was examined during and after earthquake. First, a liquefaction analysis was conducted to evaluate the effect of liquefaction countermeasure during the earthquake. Then, a consolidation analysis was conducted to evaluate ground deformation caused by dissipation of excess porewater pressure. To verify the effects of the countermeasure, the analysis results of the grid-type improved ground were compared with non-improved ground and chemical grouting improved ground. As a result, a deformation reducing effect equivalent to that of the chemical grouting improvement was obtained from the grid-type improvement. It was shown that the combination of the liquefaction analysis and consolidation analysis is useful for evaluating deformation of the ground improved by the grid-type improvement. Furthermore, the grid-type improvement with wide grid-spacing indicated an effect on reducing subsidence.

Keywords: liquefaction countermeasure, grid-type improvement, chemical grouting method, asphalt pavement

1. Introduction

It involves constrains associated with facility operation time and space when conducting liquefaction countermeasure against existing airport basic facilities, because they are in service. Types of liquefaction countermeasure methods that may be performed are also limited due to ground conditions and cost effectiveness. Sand compaction pile method is one of the density increase methods which requires large machines, and because of limited facility operation time or space, it cannot be applied in our study. Compaction grouting method, which is another kind of density increase construction method, does not require large machines, however, it is unsuitable under such conditions where overburden is thin or underground structures such as drain pipe exist because it involves displacement of the surrounding ground. Although solidification method by permanent liquid grouting does not induce displacement of the surrounding ground, it is difficult to inject chemical liquid in sandy soils containing fines. Grid-type improvement method is a method which places cement solidifications in a grid pattern and reduces the rate of improvement area, marking it cost effective. For this reasons, it is considered necessary to develop liquefaction countermeasure by grid-type improvement for airport basic facilities.

Over the course of transition to performance design method, increased focused has been on the residual deformation after earthquake. In design of port and airport structures, effective stress analysis code FLIP [1] has been widely used as a method for evaluating the seismic performance. However, in general, multi-spring model of FLIP, which is used under undrained condition based on the assumption that no flow of porewater from soil skeleton during an earthquake occurs, does not consider volumetric shrinkage caused by dissipation of excess porewater pressure the earthquake motion generates. According to the airport civil engineering facility seismic design guidelines [2], it is necessary to evaluate flatness after earthquake at airport basic facilities of wide and flat shapes. Volume shrinkage due to dissipation of excess porewater pressure also needs to be evaluated in addition to the residual deformation. There are several methods to evaluate residual deformation caused by dissipation of excess porewater pressure. One method is to calculate the amount of volume shrinkage in the liquefied sand layer from chart [3] obtained from laboratory tests. Another is to calculate by soil water coupled analysis (hereinafter, consolidation analysis called). Many liquefaction countermeasure methods including sand compaction pile method, compaction grouting method [4, 5, 6], and chemical grouting method [6, 7] have been verified with the latter analysis method, however, there is no verification analysis conducted for grid-type improvement.

Based on these facts, this study proposes a modeling and boundary condition in finite element method in order to evaluate the grid-type improvement by earthquake response analysis and consolidation analysis. Then residual deformation of airport pavement is compared with ground improvement by chemical grouting method in order to confirm countermeasure effect of grid-type improvement against airport basic facilities during earthquakes.

2. Current state of numerical analysis method of grid-type improvement

There are some references [8, 9, 10] on numerical analysis that target the grid-type improvement. Although most of them employed two-dimensional effective stress analysis (analysis code FLUSH[11] or FLIP), grid-type improvement is a three-dimensional shape. As shown in Fig.1, an in-plane wall of a body improved by reducing stiffness and the elements of unimproved ground are superposed to take account of the depth improvement ratio of the improved body. This method enabled a three-dimensional model to be applied to a two-dimensional mode by combining the in-plane wall and out-plane wall. This method also considers bending of the out-plain wall.

To evaluate the residual deformation, it is necessary to use the FLIP based on the effective stress method which is able to consider excess porewater pressure. In a self-weight analysis to calculate the initial stress before the earthquake, the liquefaction layer with small rigidity and large deformation is different from the improved body with large rigidity and small deformation in vertical displacement. Therefore, the initial stress of the liquefaction layer due to restraint of the liquefaction layer's displacement is underestimated. In order to solve this problem, both of references [9] and [10] set duplicate panel points on the improved body, the border and just above ground as a boundary condition. Duplicate panel points are able to freely displace in vertical direction, and conjugation is set equal to displacement in the horizontal direction. In dynamic analysis, there are two cases.

One case sets conjugation which meets the same displacement in horizonal and vertical direction [9]. The other case sets conjugation only in horizontal direction to represent the slipping of the improved body and ground [10]. These cases are verified focusing on excess porewater pressure of the inside or outside grating, but they do not consider any deformation. In addition, as stated above, consolidation analysis is needed to evaluate flatness after an earthquake. Therefore, some appropriate boundary conditions must be set in the consolidation analysis.

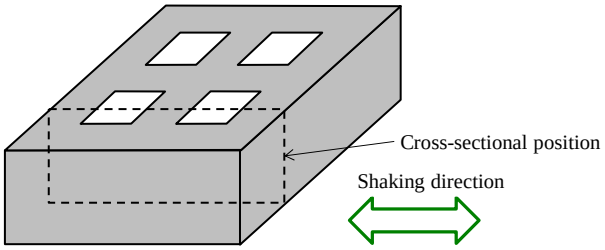

(a) Three-dimensional shape of grid-type improvement

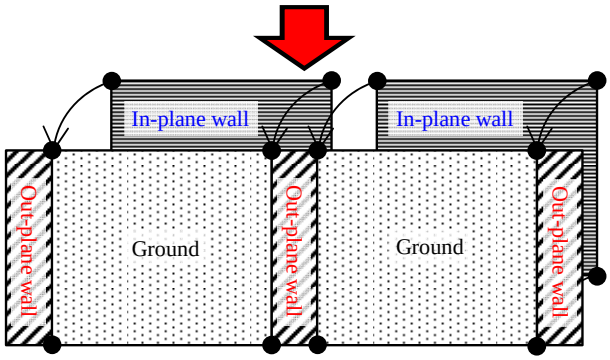

(b) Modeling method in two-dimensional grid-type improvement

Fig. 1 – Pseudo three-dimensional method

3. Analysis condition

3.1 Target ground

In October 2007, a full-scale liquefaction experiment of airport facilities was carried out in Ishikari Bay New Port [6]. In this experiment, the ground was liquefied by control blasting of an emulsion water-gel explosive in the ground. In this analysis, the ground was subjected to infiltration solidification processing, which is a solvent-based chemical grouting method. This ground was paved with asphalt similar to the runway of an airport. Further, reproduction analysis verified the experimental results. For more detailed information on reproduction analysis, reference [7] will be useful.

The physical properties of the target ground are shown in Table 1. A top view and a cross section view are shown in Fig.2. The layer shallower than 2.55m is the non-liquefaction layer, and the layer deeper than 2.55m is the liquefaction layer. A pipe (ϕ=1,000mm) was buried between these layers. After the improvement, the thickness of A-improvement was 5.4m, B-improvement was 3.6m, and C-improvement was 1.8m. These improvements are like float-type improvements because the countermeasure applies to deeper ground than the buried pipe. It should be noted that the layer shown in Fig.2 is a simplified structure to use for analysis based on the results of the ground investigation.

Table 1 – Physical properties of ground

Layer	N value (Avg.)	Liquefaction strength R_{L20}	Fine fraction content rate Fc (%)	Uniformity coefficient Uc (Avg.)	Wet density ρ_t (g/cm^3)	Consistency
Fsu Fs	1～8 (2.6)	0.189～0.244	7～38	1.7～16.8 (7.0)	1.827～1.867	NP
As1	3～12 (7.9)	-	5～22	1.9～11.0 (5.3)	-	NP
As2	8～20 (14.1)	0.204～0.222	8～32	2.4～13.2 (7.4)	1.796～1.819	NP

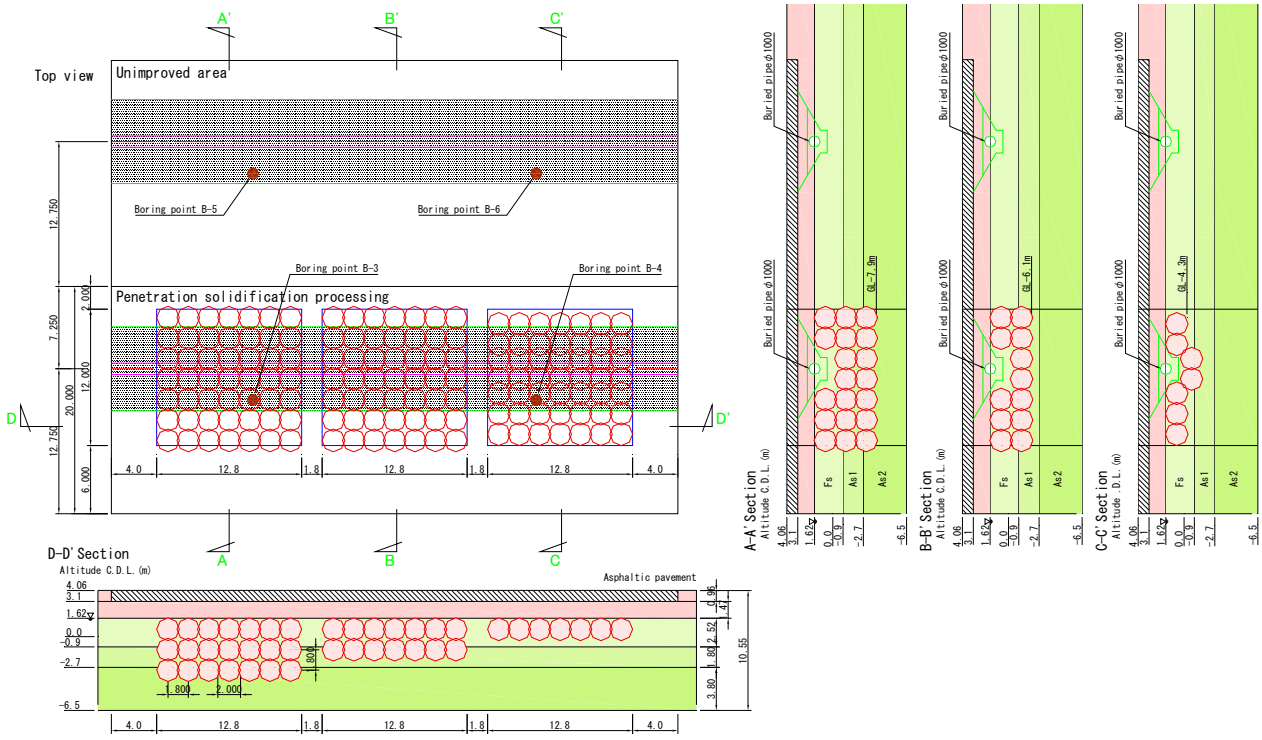

Fig 2 – Top view and a cross section view of chemical grouting

3.2 Analysis method

Two-dimensional effective stress analysis was used for earthquake response analysis, and a multi-spring model was used for representing the behavior of the sand layer under liquefaction. However, the multi-spring model in the undrained state is not able to evaluate volume shrinkage caused by dissipation of excess porewater pressure by earthquake as described earlier. Therefore, consolidation analysis was carried out after the earthquake response analysis, in order to evaluate Biot's volume shrinkage multidimensional consolidation equation, subject to stress and inflation. This is able to predict dissipation by excess porewater pressure and deformation due to dissipation. It should be noted that the consolidation analysis uses the analysis code FLIPDIS [12]. The improvement body was modeled by linear plane element.

3.3 Ground conditions

Fig.3 shows the ground model which adopted the chemical grouting method including the asphalt paving of reference [7]. The undersurface of As2 was set as the engineering foundation surface. In this study, ground models made by grid-type improvement were constructed in the same range as the range improved by chemical grouting which ensures its reproducibility. These ground models are shown in Fig.4. Further, in grid-type improvement, a mesh spacing around the improved part is half of the ground model to keep the distribution of excess porewater continuous.

The wall thickness of the improved body was set to 2m which is the same as the actual case of Sendai Airport [13]. In B-improvement, a middle wall was set and the standard grid-type spacing (L/H=0.8m) was studied. L is grid spacing, and H is improved layer thickness. The space which is considered to have an effect of decreasing excess porewater pressure is L/H=0.8 or less [14]. The details of each improvement are shown in Table 2. α is the rigidity reduction rate in the in-plane direction of the improved body to the out-plane direction of the improved body [6]. The L/H of B-improvement without a middle wall is about 2.7 times bigger than B-improvement with a middle wall.

The parameters used in the analysis are shown in Table 3, and calculated liquefaction curves are shown in Fig.5. Analysis parameters were set based on reference [7]. The parameters of liquid grouting solidification were set as reference [7], the deformation characteristics were set as the surrounding ground, and liquefaction did not occur. In the earthquake response analysis, the Rayleigh damping rigidity proportionality β was employed. Then, a ground primary natural period (0.26 seconds), a dumping ratio (1%) and the value of β (0.001) were set.

Table 2 – Details of each improvement

Improvement	L	H	L/H	Improved thickness H (m)	Rigidity reduction rate α
A	8	5.4	1.5	5.4	0.2
B (without middle wall)	8	3.6	2.2	3.6	0.2
B (with middle wall)	3	3.6	0.8		0.4
C	8	1.8	4.4	1.8	0.2

Table 3 – Parameters of analysis

Parameters			Pavement	Fsu	Fs	As1	As2	Improved body (out-plane)
Deformation characteristic	Density	ρ (g/cm^3)	2.1	1.7	1.8	1.8	1.8	1.8
	Shear wave velocity	Vs (m/s)	-	120	120	175	220	-
	Standard confining pressure	σ_{ma}' (kN/m^2)	98	98	98	98	98	-
	Shear Modulus	G_{ma} (kN/m^2)	98,900	55,300	40,100	67,000	97,100	-
	Young's modulus	E (kN/m^2)	-	-	-	-	-	882,000
	Bulk modulus	K_{ma} (kN/m^2)	258,000	144,000	105,000	175,000	253,000	-
	Poisson ratio	ν	0.33	0.33	0.33	0.33	0.33	0.26
	Porosity	n	0.41	0.53	0.53	0.53	0.53	-
	Internal friction angle	ϕ_f(deg)	40.0	38.0	37.8	39.0	40.2	-
	Maximum dumping ratio	h_{max}	0.24	0.24	0.24	0.24	0.24	-
Liquefaction characteristic	Phase transformation angle	ϕ_p (deg)	-	-	28	28	28	-
	w_1		-	-	2.488	3.000	6.000	-
	p_1		-	-	0.5	0.5	0.5	-
	p_2		-	-	1.034	0.963	0.900	-
	c_1		-	-	1.6	1.6	1.3	-
	S_1		-	-	0.005	0.005	0.005	-

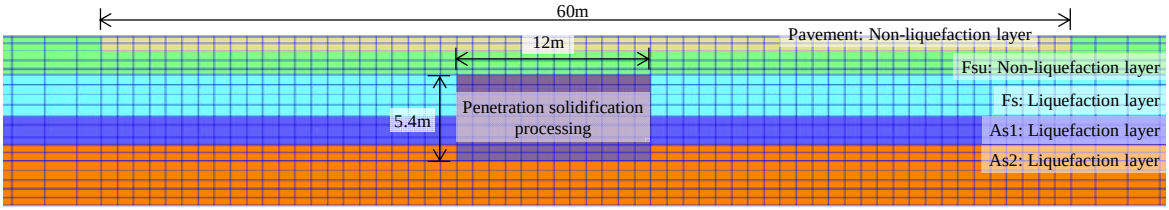

(a) A-improvement

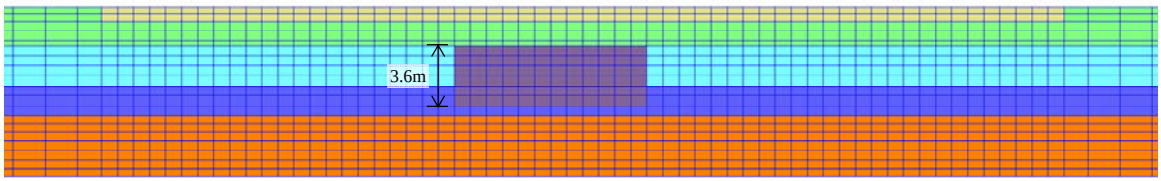

(b) B-improvement

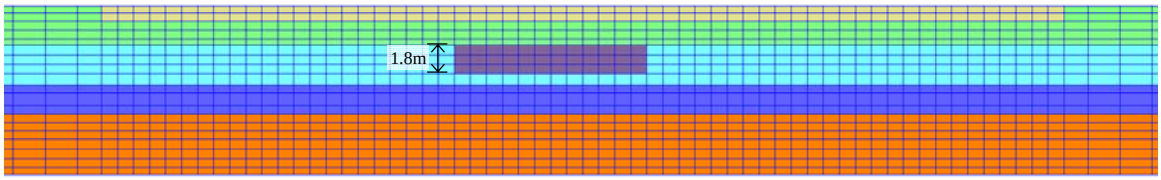

(c) C-improvement

Fig 3 – Ground model of chemical grouting

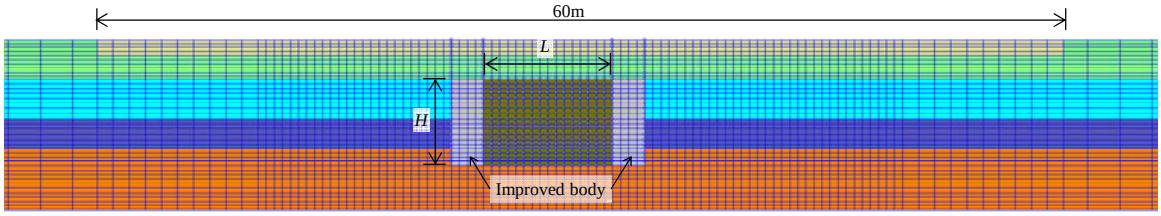

(a) A-improvement

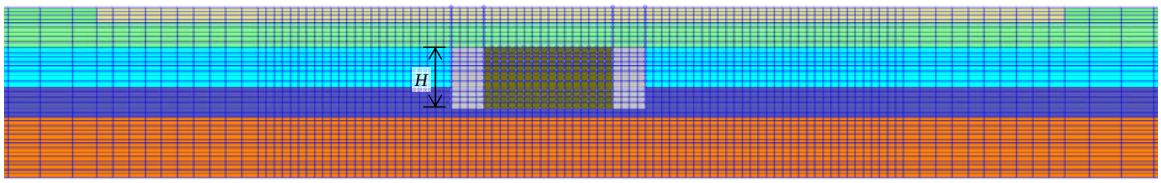

(b) B-improvement (without middle wall)

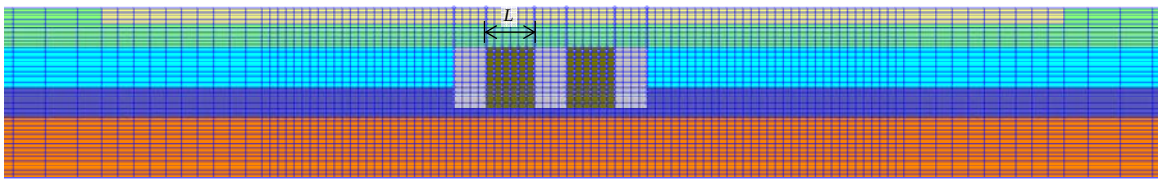

(c) B-improvement (with middle wall)

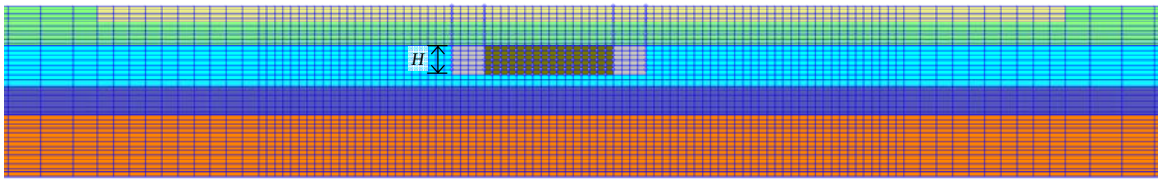

(d) C-improvement

Fig 4 – Ground model of grid-type improvement

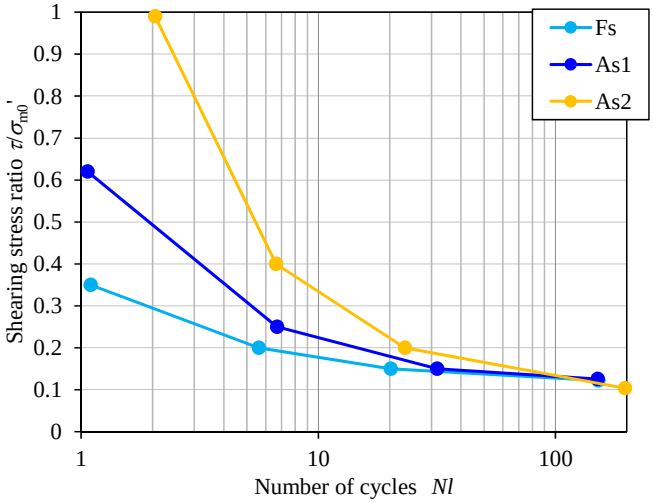

Fig 5 – Calculated liquefaction strength curves

3.4 Boundary conditions proposed in this study

This study proposes a method of setting boundary conditions for initial self-weight analysis, earthquake response analysis and consolidation analysis, for appropriate evaluation of deformation by earthquake.

The boundary conditions of self-weight analysis and earthquake response analysis are shown in Fig.6. All multi-panel points on the red frame, as shown below, were set on the ground border and just above the ground. Displacement binding in horizontal direction was applied in the self-weight analysis, and that in both directions was applied in the earthquake response analysis. This method is the same as reference [9]. The boundary conditions of consolidation analysis are shown in Fig.7. The asphalt pavement is deformed without difference in level. Without binding the liquefaction layer below the asphalt pavement, the asphalt pavement enclosed in blue is bound in vertical and horizontal direction. The layer enclosed in red is bound in only the horizontal direction. According to reference [15], voids are not generated at the bottom of the asphalt pavement. Therefore, this study assumed that the asphalt pavement is deformed following deformation of the ground.

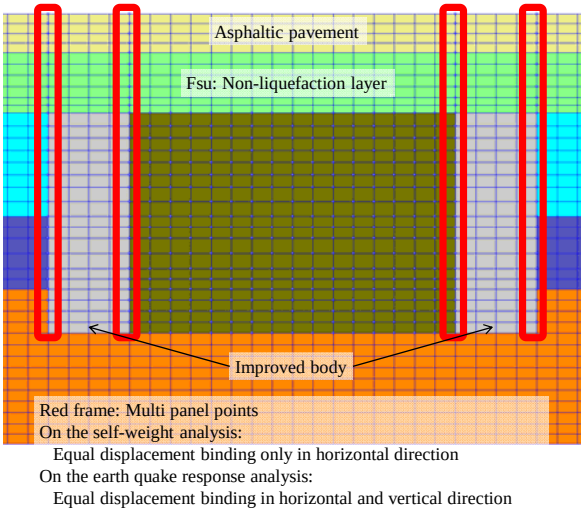

Fig 6 – Boundary condition (self-weight analysis and earthquake response analysis)

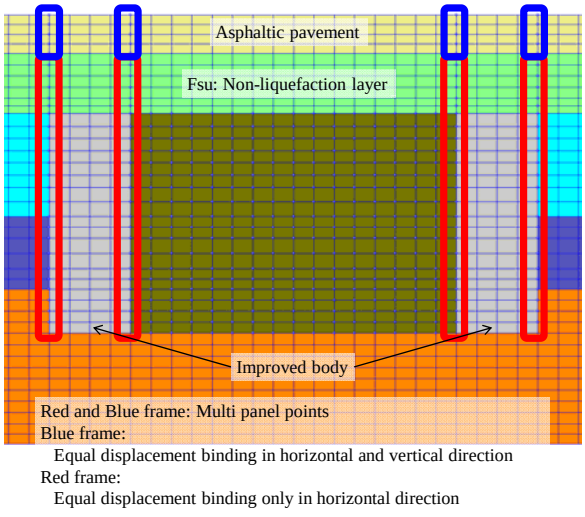

Fig 7 – Boundary condition (consolidation analysis)

3.5 Input acceleration time history

In the input acceleration time history, 5Hz frequency, 100Gal acceleration amplitude and a sine wave of 80 seconds were used as in reference [7]. It is difficult to set an appropriate acceleration waveform because a vibrational source is produced by blasting in the field experiment. The purpose of this study is not to reproduce the rise process of excess porewater pressure, but to determine the liquefaction range and distribution of excess porewater pressure for the initial state setting of consolidation analysis. Therefore this study used a sine wave. The input acceleration time history is shown in Fig.8.

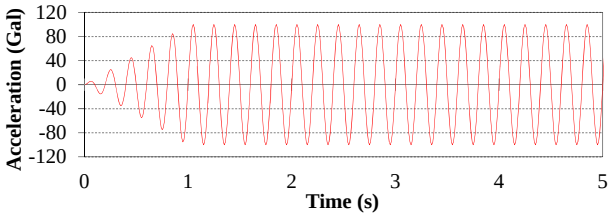

Fig 8 – Input acceleration time history

4. Results

4.1 Maximum excess porewater pressure ratio

A comparison of distribution of the maximum excess porewater pressure ratio is shown in Fig.9 through Fig.12. Excess porewater pressure ratio is a value obtained by subtracting the effective confining pressure divided by an effective confining pressure at initial self-weight analysis from 1.

Although an increase of only about 0.5is seen in most parts of As1 with non-improvement, in other grounds excess porewater pressure is increased, and the grounds seem to be liquefied in their entirety. Next, focus attention on the excess porewater pressure in the grid. It increased poorly in the center with A-improvement, B-improvement (without middle wall) and C-improvement, and increased except for the center. With B-improvement (with middle wall), it was slightly increased in the whole grid area. This was the same result as the published one [15] in that excess porewater pressure hardly increases with the standard grid-spacing, but increases with a wider grid-spacing. When focusing on excess porewater pressure in the range of non-improvement, it does not increase in some part of the ground of the improved body side of A-improvement and B-improvement, but in no part with chemical grouting. On the other hand, far from the improved range, excess porewater pressure increased both with grid-type improvement and chemical grouting compared to non-improvement. The results might have changed due to the interaction of rigidity difference between chemical grouting, grid-type improvement and non-improvement. The increase of excess porewater pressure at the bottoms of B-improvement and C-improvement was slightly suppressed with both chemical grouting and grid-type improvement.

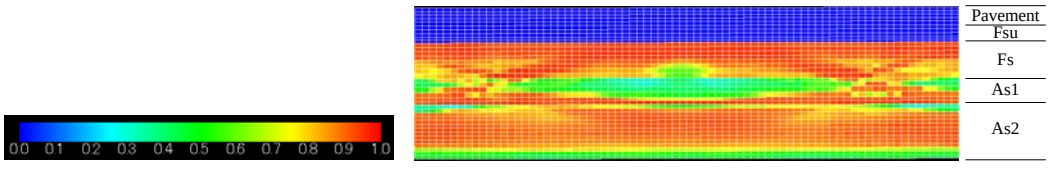

Fig 9 – Excess porewater pressure ratio distribution in non-improvement

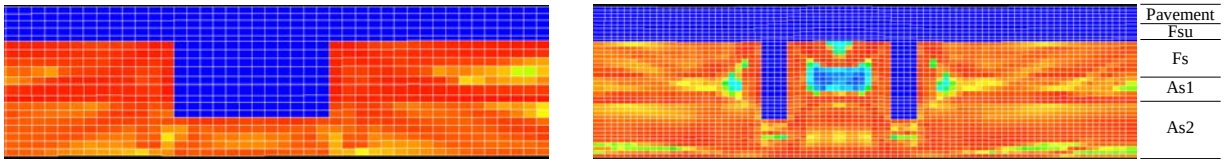

(a) Chemical grouting (b) Grid-type improvement

Fig 10 – Excess porewater pressure ratio distribution in the A-improvement

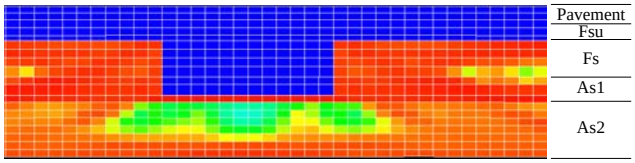

(a) Chemical grouting

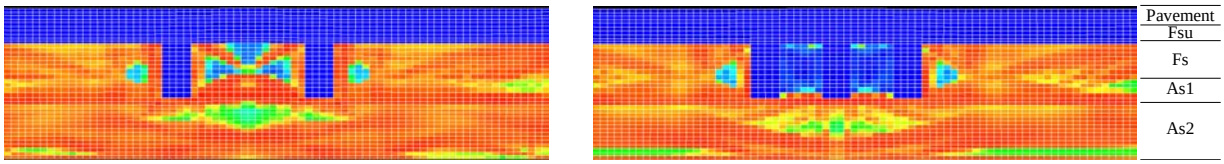

(b) Grid-type improvement (without middle wall) (c) Grid-type improvement (with middle wall)

Fig 11 – Excess porewater pressure ratio distribution in B-improvement

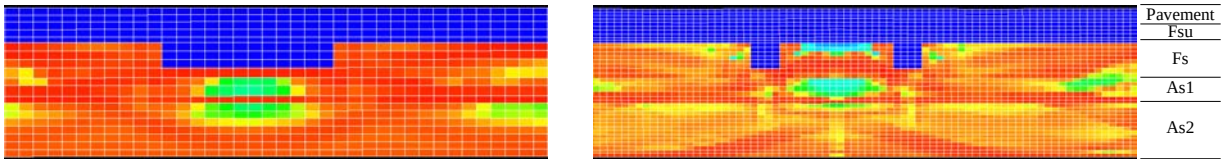

(a) Chemical grouting (b) Grid-type improvement

Fig 12 – Distribution of excess porewater pressure ratio in C-improvement

4.2 Ground surface shape distribution

The ground surface shape distribution of the paving range of A, B, and C-improvement and non-improvement grounds is shown in Fig.13. The improved range is within the yellow-green broken lines. For B-improvement, analysis results of with or without middle wall of grid-type improvement are shown together. The surface was flat before blasting, with a constant altitude of 4.06m.

Immediately after the earthquake, little difference was seen between A, B, and C-improvement, chemical grouting, and grid-type improvement, showing that subsidence due to deformation by the earthquake was small. Residual subsidence due to the earthquake was hardly generated because the ground surface is horizontal and horizontally layered, and earthquake response analysis was carried out in the undrained state. After excess porewater pressure dissipation, the subsidence of the runway center is about 25cm with non-improvement, 10cm with A-improvement, 15 to 20cm with B-improvement, 30cm with C-improvement. A-improvement and B-improvement but not C-improvement had a subsidence suppressive effect.

When comparing the methods to each other, there is little difference between chemical grouting and grid-type improvement with A, B, and C-improvement. However, the subsidence for grid-type improvement (except for B-improvement with middle wall) is slightly larger than for chemical grouting. This is because excess porewater pressure in the countermeasure range with chemical grouting was not increased, but was increased and dissipated with grid-type improvement. However, comparing chemical grouting in B-improvement and grid-type improvement with middle wall, water pressure in the improved body was not increased in either, and subsidence is smaller with grid-type improvement. This is probably because the subsidence was suppressed compared to chemical grouting as water pressure was not increased in some part of the side of the ground in grid-type improvement. Around the pavement edge, subsidence is about 27cm with non-improvement, and 35cm with A,

B, and C-improvement, which shows a tendency that subsidence is larger with ground improvement. This is possibly because, as described above, excess porewater pressure was increased and dispersed in the surrounding ground far from the countermeasure range both with grid-type improvement and chemical grouting compared to non-improvement.

When focusing on B-improvement with or without middle wall in grid-type improvement, *L/H* without middle wall (wide spacing) is about 2.7 times larger than that with middle wall (standard spacing), but subsidence is about 16cm versus 20cm, thus the subsidence is only about 1.2 times larger.

The suppressing effect of excess porewater pressure was achieved with grid-type B-improvement as with chemical grouting, and the subsidence was similar for both methods. The setting of the proposed boundary conditions in this study made it possible to express the suppression effects of grid-type improvement on excess porewater pressure and deformation of asphalt pavement on the improved ground, and it was found that those effects are comparable to chemical grouting.

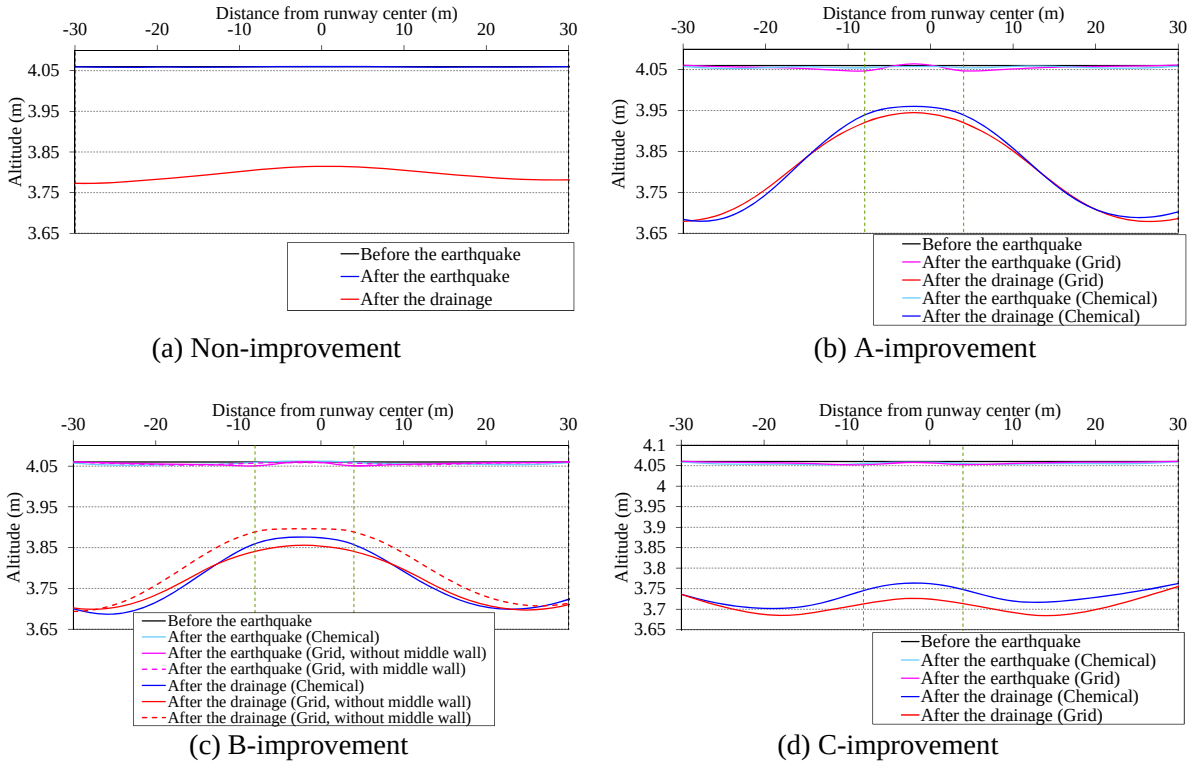

(a) Non-improvement (b) A-improvement

(c) B-improvement (d) C-improvement

Fig 13 – Ground surface shape distribution

4.3 Gradient distribution

The gradient distribution with A, B, C-improvement and non-improvement is shown in Fig.14. The green dashed lines represent the defined value for a runway cross gradient 1.5% [2].

The maximum gradient of is about 1.8% with chemical grouting and 1.6% with grid-type improvement on A-improvement, 1.4% with chemical grouting and 1.3% with grid-type improvement on B-improvement, and 0.7% with chemical grouting and 0.3% with grid-type improvement on C-improvement. A value exceeding the prescribed gradient was obtained in both chemical grouting and grid-type improvement in A-improvement which has a large reducing effect on subsidence. However, the prescribed gradient was satisfied in the improved range and under other improvement conditions. As a result, a trend was observed that the gradient increased as the subsidence was suppressed.

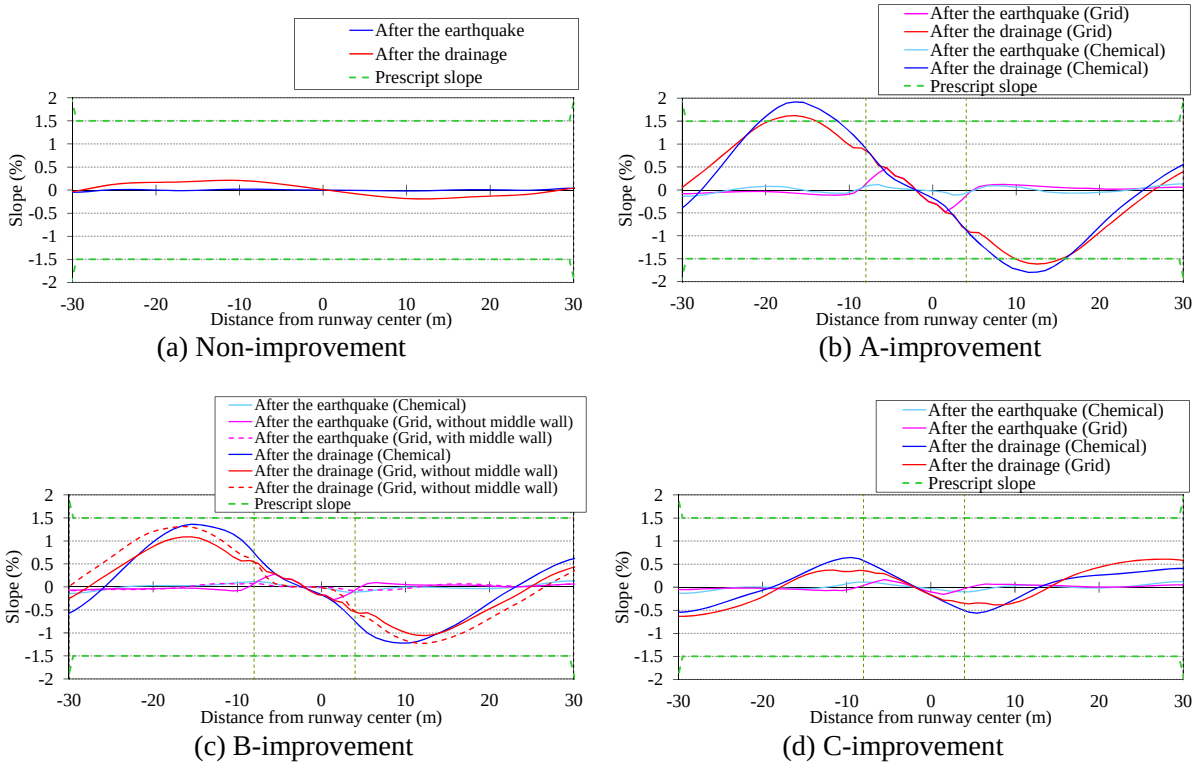

Fig 14 – Gradient distribution

5. Conclusion

In this study, numerical analyses were conducted to make sure the effect of the grid-type improvement using the ground model based on a full-scale blast experiment at Ishikari Bay New Port. Then the results of the grid-type improvement before and after dissipation of excess porewater pressure were compared with those of the ground improved by the chemical grouting method. The following conclusions were obtained:

(1) It is possible to evaluate deformation of ground improved by grid-type improvement after an earthquake using combined seismic response and consolidation analysis with the proposed boundary conditions depending on analysis type.

(2) In the case of standard grid-spacing, it is possible to suppress the generation of the excess porewater pressure inside of the grids. Then displacements and declination of the asphalt pavement decrease under a minimal value to satisfy seismic performance, resulting in a reduction effect same as the chemical grouting method according to the improved ground area.

(3) If grid-spacing is widened more than the standard grid-spacing in grid-type improvement, generation of excess porewater pressure cannot be suppressed perfectly but a reducing effect on subsidence is obtained. For instance, when the grid-spacing is set to 2.7 times of the standard grid-spacing, subsidence of the asphalt pavement increases only 1.2 times more than in the case of the standard grid-spacing.

6. Acknowledgments

Dr. Katsuya Ikeno (Penta-Ocean Construction Co., Ltd.) provided us material for the analysis. We would like to express our appreciation here.

7. References

[1] Iai S, Matsunaga Y, and Kameoka T (1990): Parameter identification for a cyclic mobility model, *Report of the Port and Harbour Research Institute*, Vol.29, No.4, pp.57-83.

[2] Ministry of Land, Infrastructure, Transport and Tourism Civil Aviation Bureau, National Institute for Land and Infrastructure Management supervision, Port and Airport Research Center (2013): *Airport Civil Engineering Facility Seismic Design Guidelines and Design Example*. (in Japanese)

[3] Ishihara K, and Yoshimine M (1992): Evaluation of settlements in sand deposits following liquefaction during earthquakes, *Soil and Foundation*, Vol.32, No.1, pp.173-188.

[4] Ukita Y, Shiga M, Moroboshi K, and Tokoro M (2007): Liquefaction countermeasure range in runway and taxiway, *Report of the Coastal Development Institute of Technology*, No.7, pp.69-72. (in Japanese)

[5] Takahashi H, Oohashi T, Endo T, Fujii T, Kaneko T, and Mizuno S (2013): Test execution and numerical analyses of static compaction grouting method to reduce improvement ratio, *Japanese Geotechnical Journal*, Vol.8 No.3, pp.451-461. (in Japanese)

[6] Sugano T, and Nakazawa H (2009): Experimental Study on Countermeasures for Liquefaction subjected to Full-Scale Airport Facilities, *Technical Note of the Port and Airport Research Institute*, No.1195. (in Japanese)

[7] Sugano T, Nakazawa H, Ikeno K, and Mitou M (2010): Study on Countermeasure for Liquefaction to Runway Ground by Application of Chemical Grouting Method, *Technical Note of the Port and Airport Research Institute*, No.1206. (in Japanese)

[8] Taya Y, Uchida A, Yoshizawa M, Onimaru S, Yamashita K, and Tsukuni S (2008): Simple method for determining lattice intervals in grid-form ground improvement, *Japanese Geotechnical Journal*, Vol.3 No.3, pp.203-212. (in Japanese)

[9] Yoshida M, Takahashi H, Morikawa Y, Fukada H, Nakajima H, Kawata M, Mizutani S, and Sumiya K (2013): Pseudo-3d analyses method of floating lattice-shaped cement treatment and its applicability for horizontally-layered ground, *Journal of Japan Society of Civil Engineers*, Vol.69 No.2, pp.I_958-I_963. (in Japanese)

[10] Saeki Y, Ohya Y, Kohama E, and Sugano T, (2013): Reproducible analysis of model vibration experiment intended for the grid-type improvements in airport pavement, *48th Japan National Conference on Geotechnical Engineering*. (in Japanese)

[11] J Lysmer, T Udaka, CF Tsai and HB Seed (1975): FLUSH-A computer program for approximate 3-D analysis of soil-structure interaction problems, Report No. EERC75-30, University of California, Berkeley.

[12] Morio S, and Tohyama M: FLIPDIS (post-processing program of liquefaction analysis program FLIP), http://www.ptmsg.net/product/flipdis/index.html, Browsed on September 4, 2014 (in Japanese)

[13] Shinohe S (2008): Sendai Airport earthquake resistance ground improvement work, *9th Airport Technical Report Conference*. (in Japanese)

[14] Ministry of Construction Public Works Research Institute (1999): *Liquefaction Countermeasure Method Design and Construction Manual (Draft)*, No.186, pp.478. (in Japanese)

[15] Ohya Y, Kohama E, Sugano T, Imai M, Higashinaka K, and Saeki Y (2014): Shake table test on deformation characteristic of asphalt pavement above grid-type improvement with wide grid spacing, *Journal of Japan Society of Civil Engineers*, Ser. A1, Vol. 70 No. 4, pp. I_227-I_241 (in Japanese)